PLOS ONE

RESEARCH ARTICLE

Molecular crypsis by pathogenic fungi using human factor H. A numerical model

Stefan N. Lang[1], Sebastian Germerodt[1], Christina Glock[1], Christine Skerka[2], Peter F. Zipfel[2,3], Stefan Schuster[1]*

1 Dept. of Bioinformatics, Friedrich Schiller University Jena, Jena, Germany, **2** Dept. of Infection Biology, Leibniz Institute for Natural Product Research and Infection Biology - Hans Knöll Institute, Jena, Germany, **3** Institute of Microbiology, Friedrich Schiller University Jena, Jena, Germany

* stefan.schu@uni-jena.de

Check for updates

OPEN ACCESS

Citation: Lang SN, Germerodt S, Glock C, Skerka C, Zipfel PF, Schuster S (2019) Molecular crypsis by pathogenic fungi using human factor H. A numerical model. PLoS ONE 14(2): e0212187. https://doi.org/10.1371/journal.pone.0212187

Editor: Elizabeth S. Mayne, University of Witwatersrand/NHLS, SOUTH AFRICA

Received: May 28, 2018

Accepted: January 29, 2019

Published: February 19, 2019

Copyright: © 2019 Lang et al. This is an open access article distributed under the terms of the Creative Commons Attribution License, which permits unrestricted use, distribution, and reproduction in any medium, provided the original author and source are credited.

Data Availability Statement: All relevant data are within the paper and its Supporting Information files.

Funding: This work was supported by the German Research Foundation (DFG) within the Jena School for Microbial Communication (grant no. DFG-GSC 214/2) and the Transregio 124 (FungiNet, projects B1, C4 and C6).

Competing interests: The authors have declared that no competing interests exist.

Abstract

Molecular mimicry is the formation of specific molecules by microbial pathogens to avoid recognition and attack by the immune system of the host. Several pathogenic Ascomycota and Zygomycota show such a behaviour by utilizing human complement factor H to hide in the blood stream. We call this type of mimicry molecular crypsis. Such a crypsis can reach a point where the immune system can no longer clearly distinguish between self and non-self cells. Thus, a trade-off between attacking disguised pathogens and erroneously attacking host cells has to be made. Based on signalling theory and protein-interaction modelling, we here present a mathematical model of molecular crypsis of pathogenic fungi using the example of *Candida albicans*. We tackle the question whether perfect crypsis is feasible, which would imply that protection of human cells by complement factors would be useless. The model identifies pathogen abundance relative to host cell abundance as the predominant factor influencing successful or unsuccessful molecular crypsis. If pathogen cells gain a (locally) quantitative advantage over host cells, even autoreactivity may occur. Our new model enables insights into the mechanisms of candidiasis-induced sepsis and complement-associated autoimmune diseases.

Introduction

Crypsis and mimicry are wide-spread phenomena in biology. They are used to deceive predators, prey, hosts or other interaction partners. Most commonly they are used as defensive strategies like imitation of harmful species by harmless species (Batesian mimicry) or imitation of a dominant element of the environment (cryptic mimesis) [1–3]. Aggressive mimicry refers to the observation that some predators use camouflage not to be recognized by their prey. Mimicry can also be useful for reproduction, for example, in egg mimicry realized by some birds [1–3]. The effect of mimicry can be understood by analogies from human society. For example, uniforms may be misused by civilians, as was impressively described in the movies "The Sting" and "Catch Me If You Can" and in the theatre play "The Captain of Koepenick" by Carl

Zuckmayer [4]. Transferred to our example of molecular mimicry, micro-organisms imitate the appearance of host cells by mimicking molecular key factors of their cell surfaces.

Crypsis and mimicry require three entities: a model (in the case of crypsis this is the environment) which is imitated by a mimic to deceive a dupe (also called operator). Usually mimicry systems are discussed with respect to animals and plants [5–7], but they also occur in the realm of pathogenic micro-organisms. Besides visual features, the mimicked trait is often a chemical compound. For example, when predatory animals roll on the grass to hide their odour from potential prey. Damian [8] introduced the term "molecular mimicry" to describe antigen sharing between host and parasites. Later Damian [9] loosened its definition to the microbial production of "similar or shared molecular structures", preventing host response.

Also nowadays, molecular mimicry research focuses mainly on the adaptive immune system [10–13]. In this paper an example of molecular crypsis by pathogenic fungi so as to deceive innate immunity is studied, notably the recruitment of a special human immune regulatory protein, the complement factor H (FH). This is performed by various fungal pathogens such as *Candida albicans* [14], *Staphylococcus aureus* [15] or *Borrelia burgdorferi* [16–19]. We perform our analysis using the example of *C. albicans* although the utilization of human complement regulatory proteins to avoid complement attack is a general phenomenon and the analysis is easily adaptable to be applied to other pathogens.

The presented model analyses the initial phase of activation of the alternative pathway of the human complement system [20]. The complement system is a part of innate immunity, which is not adaptable and does not change over the course of an individual's lifetime. Complement consists of several molecular components which are circulating as inactive precursors in the blood. When stimulated by a trigger, complement gets activated and aids in removal of the intruder. We assume the host not to tolerate any micro-organisms in the blood-stream. This is in contrast to other compartments like the apical sides of alveoli, intestine, skin, etc., where niches for beneficial micro-organisms are provided.

Key factors of the complement system are FH together with complement component 3 (C3) [20]. Both are continuously present at high concentrations in the blood. C3 is cleaved to C3b, which can bind covalently to the surface of host and pathogen cells [21–23]. Together with complement factor B and activated by factor D, C3b can form the C3b convertase (C3bBb), again converting C3 into C3b, so that a local amplification of C3b generation by a positive feedback loop occurs (see Fig 1).

The accumulation of C3b on the cell surface is called opsonization. The deposited C3b on the surface acts as a signal for phagocytes, like macrophages, to remove the tagged cells. Additionally opsonization with C3b has various downstream effects on the innate, as well as the adaptive immune system. For example, it mediates the formation of a terminal complement complex (TCC) at a high opsonization state, effectively perforating the cell membrane and triggering lysis of the cell [23].

C3b binds to all types of surfaces, both self and non-self [21]. The discrimination between self and non-self is accomplished by FH and other complement regulators [24]. FH can bind to glycosaminogens on the host surface, like heparan sulfates and to surface deposited C3b. Once bound to the cell surface, FH prevents C3b amplification and is able to inactivate surface-bound C3b. For damaged host cells, C-reactive protein (CRP) can prevent binding of FH to the cell surface, thus maintaining opsonization [23, 24]. The main expression site of FH and C3 is the liver, but local expression can be accomplished by other cell lines as well, for example, (in the case of FH) endothelial, epithelial or muscle cells [25, 26].

Molecular crypsis enters the scene in that several pathogenic fungi and micro-organisms bind FH or other complement regulators by, for example, the complement regulators acquiring surface proteins (CRASP), like pH regulated antigen (Pra1) of *C. albicans* and other

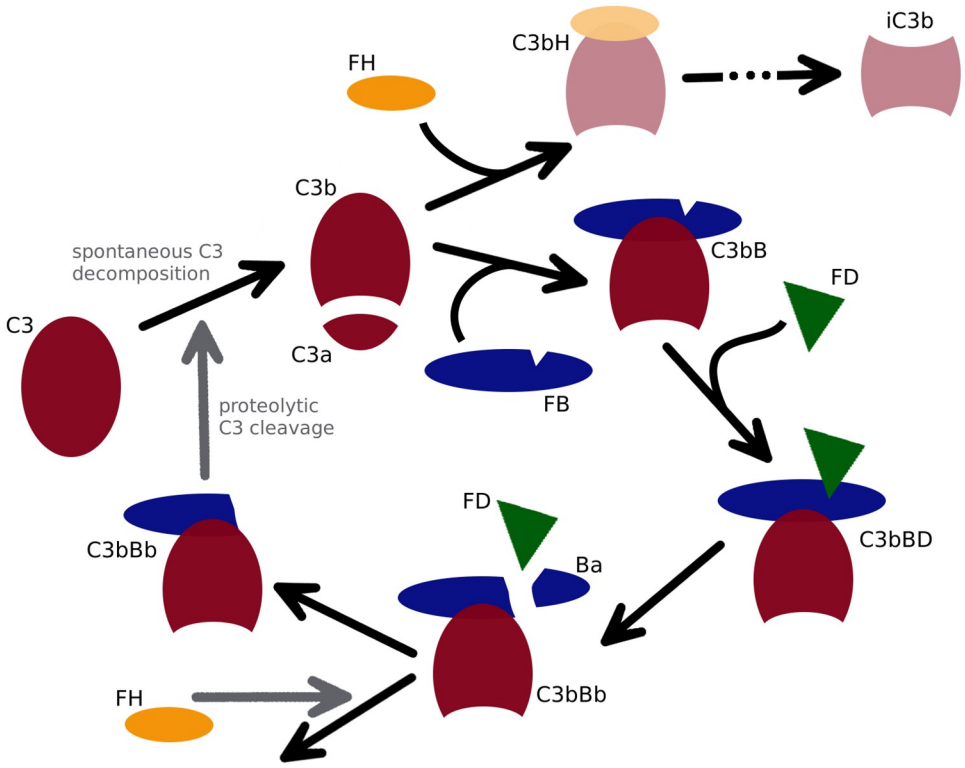

Fig 1. Generalized scheme of C3b amplification and regulation. C3b activation can occur in fluid phase or on surface. Under physiological conditions, C3b amplification in fluid phase is prevented by FH. On cell surfaces, amplification may occur, depending on whether or not FH can be acquired there. If FH cannot be acquired in sufficient amounts, there is a steady but slow conversion of C3 to C3b initiating amplification. C3b then associates with factor B (FB) to form the C3 proconvertase (C3bB), which is activated by factor D, resulting in the active C3 convertase (C3bBb). C3bBb in turn is able to proteolytically convert C3 into C3b at a high rate, starting the loop again and thus acting as an amplifier of C3b production. The amplification loop can be controlled by FH at two stages. Firstly, FH competes with FB for C3b binding, acting as a cofactor for C3b degradation to iC3b. Secondly FH is able to accelerate the decay of C3bBb, reducing proteolytic C3b generation.

https://doi.org/10.1371/journal.pone.0212187.g001

proteins [14–19]. FH recruitment to the pathogen surface could then prevent C3b opsonization, as it does for host cells. The opaque form of *C. albicans* [27–29] is additionally able to degrade C3 and C3b directly using for example the endopeptidase SAP1. This may enhance or enable FH-independent crypsis of the pathogen. In this manuscript, we focus mainly on the white form, which does not express SAP1 [30].

As the difference in C3b deposition on host and pathogen cells decreases, phagocytes may have more trouble to discriminate between self and non-self. In consequence, the host may have to decide on a trade-off between erroneously attacking own cells, possibly inducing autoreactivity, and the effectiveness by which it is able to clear mimetic pathogens from the blood (see Fig 2). This trade-off may not always be easy to find, which might be related to the presence of two different FH alleles in the human population, one leading to a higher risk of autoreactivity than the other [31, 32]. This illustrates the role of complement as a 'double-edged sword' [33–35] where the immune system may erroneously attack own cells and, on the other hand, pathogens may mimic host cells as an evasion strategy (see [36] for alternative evasion strategies).

One may have different opinions on which phenomenon occurs. Pasteur [2] doubts relationships of molecular mimicry to organismic mimicry because in the former case there is "no

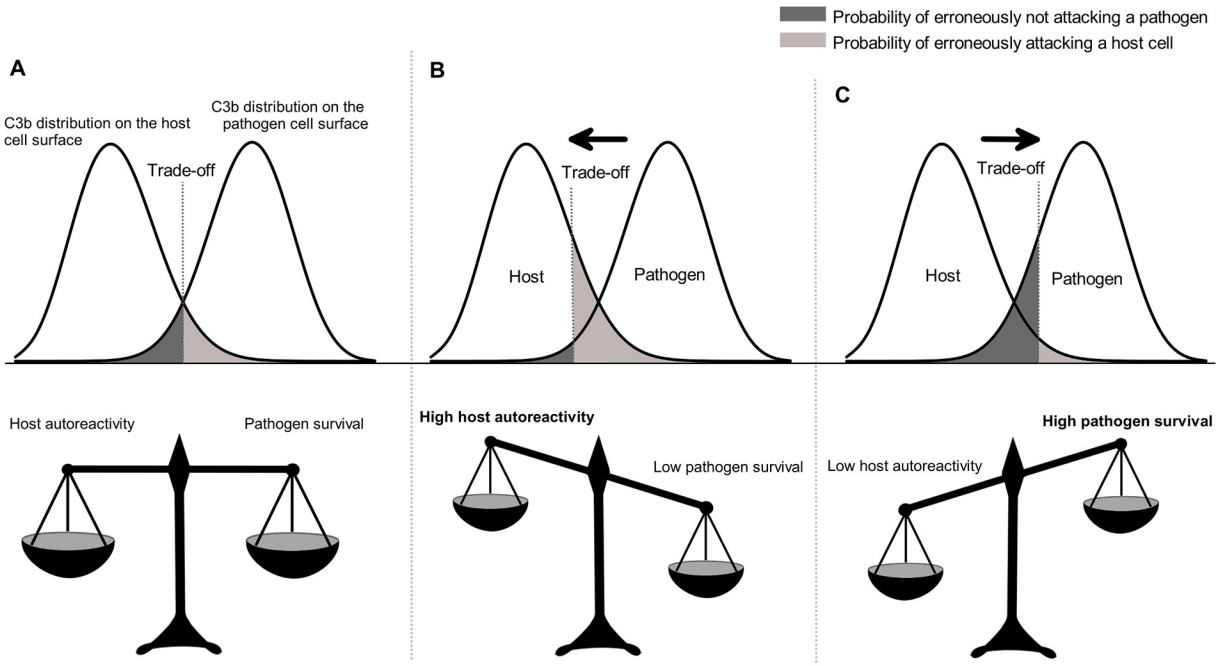

Fig 2. Example C3b distributions with differently weighted trade-off. This figure illustrates the attack decision problem the host faces for different C3b distributions on host and pathogen cell surfaces. All cells with a higher amount of C3b bound to the cell surface than the threshold will be attacked. (A) Equally weighted trade-off; the probability of erroneously attacking a host cell is equal to the probability of erroneously not attacking a pathogen cell. (B) Trade-off weighted in favour of the effectiveness in clearing mimetic pathogens. (C) Trade-off weighted in favour of low autoreactivity.

https://doi.org/10.1371/journal.pone.0212187.g002

sensory perception involved". Nevertheless in the case of molecular mimicry antigens are bound by antibodies which activate Fc-receptors on the surface of phagocytes. Also in the case of (unsuccessful) molecular crypsis, various receptors are activated. Activation of those receptors triggers specific signalling pathways, leading to a specific response of the phagocytes. Thus we adopt the view that a molecular equivalent of sensory perception is involved and molecular mimicry should be analysed like any other mimicry system. Furthermore we consider FH recruitment to prevent C3b opsonization as a new type of molecular mimicry with the difference that instead of mimicking a specific antigen (actively transmit a self signal), pathogens prevent deposition of specific opsonins to camouflage in the environment of the blood-stream (actively inhibit a non-self signal).

Accordingly, we classify this system as molecular cryptic mimesis (molecular crypsis), involving the unusual case that the environment is not neutral to the dupe. This is because the environment is a multicellular organism to which the dupe (phagocytes) belongs. When pathogens use camouflage, they make, for phagocytes, the decision of whether or not to attack cells very hard because it may happen that own cells are attacked.

Host-pathogen interactions have been successfully analysed by mathematical modelling [37–40] In particular, mathematical models describing mimicry by using, for example, methods from game theory, have been presented earlier for higher organisms, either in a general context [6, 7, 41] or for specific types of mimicry [42, 43]. In contrast, models describing molecular mimicry of bacteria or fungi are rare. Our paper is aimed at filling this gap and extending theoretical mimicry research to pathogenic micro-organisms including fungi. This helps us provide an alternative view on a wide variety of complement-associated autoimmune diseases, including the ambiguous or paradoxical role complement plays in the pathogenesis

of sepsis, which is an exaggerated inflammation and a multifactorial disease. Despite its role in protection, complement can also contribute to the development of severe complications in sepsis, notably injury to host tissues and organs [44].

The question arises whether the pathogen is capable of perfect mimicry (camouflage). In that situation, the human immune system would not be able to distinguish between human cells and pathogen cells. Then, however, protection of human cells by complement factors would be useless. On the other hand, complement factors are successfully used. Our study is aimed at investigating how the immune system can resolve that paradox.

Materials and methods

We start by analysing the attack-decision problem the host faces. Based on a single trait, which is here opsonization with C3b, phagocytes have to decide whether or not to attack a single cell, being either a host cell or a pathogen. As a result of this decision two errors may arise: erroneously attacking a host cell and erroneously not attacking a pathogen. Using an approach to study mimicry in higher organisms [7, 41], we can quantify each of the errors, depending on the encounter rate and the pathogenity of the intruder and the aggressiveness of the host's immune system (above which threshold of C3b opsonization the host attacks). Based on those errors, their respective probabilities and their severity, we use a population-based evolutionary model to outline the key parameters which influence molecular crypsis in a general context.

In the second part, we examine opsonization states of an individual infection scenario. This is done by adapting a model of human complement system [45, 46] to account for FH recruitment of pathogenic microbes. For the additional parameter values, experiments were performed (S1 and S2 Tables). Our adapted model is used to predict physiological C3b opsonization states for the two microbial species *Candida albicans* and *Escherichia coli*, each in comparison to human erythrocytes. It is worth mentioning that *E. coli* is able to perform molecular crypsis, utilizing for example the C4b-binding protein, which may also have C3b-degrading function [47]. However, to our knowledge, it is not able to utilize FH. We further generate C3b distributions for a single infection with one of the two microbes, which are then used to analyze possible strategies the host could adopt to react to molecular crypsis of pathogens. Thus, we consider *E. coli* for comparison to *C. albicans*, to include a cell type that does not perform molecular crypsis using FH. Note that it is not necessary to distinguish between pathogenic and non-pathogenic *E. coli*.

For simplicity we did not consider infection with multiple pathogens at the same time in this model. This does not severely limit the value of our model because the decision problem for the host remains self versus non-self. Combined infection with multiple pathogens could be modelled by grouping all infecting species into a "non-self" group and the usage of combined (multimodal) distributions for the parameters of this group (with modes centered at the species-specific parameters).

The following modelling approaches share the same basic assumptions about complement dynamics which will be briefly summarized here. C3b attaches equally to all cell surfaces present in the blood. Once bound, it may amplify on the cell surface. This leads to deposition of high amounts of C3b, which acts as a signal for phagocytosis or directly triggers lysis of the cell. Deposition of C3b can be prevented by recruitment of FH to the cell surface. The host can only distinguish between self and non-self if the difference in C3b deposition is sufficiently high. This way, pathogens which are able to acquire FH on their cell surface (by producing the appropriate binding receptors) may be able to camouflage as host cells.

Computing distributions of surface-bound FH

The binding reaction of FH (denoted H here) to a binding site B in a fixed-volume reaction vessel can be described in an approximative way by the following reaction equation:

$$\mathrm{H} + \mathrm{B} \underset{k_-}{\overset{k_+}{\rightleftharpoons}} \mathrm{HB}, \tag{1}$$

where k_+ and k_- are rate constants. We use this reaction equation to approximate the binding of FH to the host cell surface, although the localisation of the binding sites on the surface induces spatial effects, which we consider later. Let H and HB denote the number of free and bound FH molecules, respectively, and B the number of free binding sites. Then, for the mean dissociation constant K_d of all molecules binding FH on the cell surface, we have

$$K_d = \frac{H \cdot B}{HB} = \frac{k_-}{k_+}. \tag{2}$$

Defining n as the total number of all binding sites on pathogen surfaces in the medium, i.e.

$$n = B + HB, \tag{3}$$

it follows for the dissociation constant

$$K_d = \frac{H \cdot (n - HB)}{HB}. \tag{4}$$

This can be rewritten as

$$\frac{H}{K_d + H} = \frac{HB}{n} \equiv p, \tag{5}$$

where we define the variable p for the fraction of occupied binding sites, or, the probability that a single binding site is occupied. For the immune system, it is of interest how many of all binding sites are occupied. This number is here denoted by k. The binomial distribution applies because that corresponds to the number of k-combinations from a given set of n elements:

$$\mathcal{B}(k|p,n) = \binom{n}{k} p^k (1-p)^{n-k} \tag{6}$$

$$= \binom{n}{k} \left(\frac{H}{K_d + H}\right)^k \left(\frac{K_d}{K_d + H}\right)^{n-k}, \tag{7}$$

Note that $n - k$ binding sites are not occupied. The expected value μ and the standard deviation σ of this distribution are

$$\mu = np = \frac{nH}{K_d + H}, \tag{8}$$

$$\sigma = \sqrt{np(1-p)} = \frac{\sqrt{nHK_d}}{K_d + H}. \tag{9}$$

Note that we can generally assume large n on the host side, but also on the pathogen side if cell numbers are high enough. For large n the binomial distribution may converge to a Poisson distribution ($p \to 0$) or a normal distribution, as depicted in Fig 2.

Defining the attack decision

Approximation of the attack decision follows the theoretical work of Holen and Johnstone [7] on mimicry systems and the work of Wiley [48] on signal perception in biological systems.

Given a particular C3b opsonization state k, the decision of attacking can be made by the host using any function, for example a sigmoid, where all trait values k above a certain threshold t will be attacked. For simplicity we will assume a step function. This implies that once a cell is opsonized sufficiently, there will be no chance evading phagocytosis or lysis.

Given a threshold t the two errors arising can be quantified using the cumulative distribution functions $\mathcal{F}_H$ and $\mathcal{F}_P$ of the C3b distribution of host and pathogens. This distribution depends inversely on the distribution of surface bound FH derived above and is quantified with real-world data in the protein-interaction model later. That is, $\mathcal{F}_H(t)$ is the probability of erroneously attacking a host cell and $1 - \mathcal{F}_P(t)$ is the probability of erroneously not attacking a pathogen.

If there is no further information on the two signal distributions, signalling theory suggests the optimal way of discriminating the signals to be minimisation of a linear combination of these two errors, where the weights depend on the encounter probabilities, which are proportional to the respective cell numbers [7, 48]. It should be considered that in the case of infection by a pathogen, the weighting factors may be time-dependent because the cell numbers of pathogens vary. Thus, it would be beneficial to adjust the threshold during inflammation. It has indeed been observed that autoreactivity and inflammation are correlated [49]. We consider this effect in that the optimal threshold depends on pathogen abundance.

Moreover, in systems where the attack decision implies some benefit or cost, depending on whether it was right or erroneous, the probabilities of the two errors should additionally be weighted by the benefit in correctly attacking a pathogen and the costs arising by erroneously attacking an own cell [48]. The more virulent a pathogen is, the higher is the benefit of attack.

Taking all together, in the presented model, it is beneficial for phagocytes to choose a threshold t^*, where the difference of the probability of attacking a pathogen, weighted by the benefit B and the probability of attacking an own cell weighted by the cost C is maximized:

$$f_A(t) = (1-p)\mathcal{F}_P(t)B - p\mathcal{F}_H(t)C \tag{10}$$

Note that in this formula, we assume an infection with a single pathogen, so the encounter probability of the pathogen can be approximated by $(1 - p)$ with p being the encounter probability of the host. A more exact model should not only include the frequency- but also the density dependency.

Assuming a normally distributed trait value with standard deviation σ (note that for high receptor numbers the binomial C3b distribution converges to a normal distribution) Holen and Johnstone [7] identified the optimal attack threshold for this type of fitness function to be:

$$t^* = \frac{m}{2} - \frac{\ln(K)\sigma^2}{m}, \qquad \text{where } K = \frac{pC}{(1-p)B} \tag{11}$$

In this formula m is the distance in the trait value space of both species. Smaller m values indicate better mimetic resemblance and generally result in a higher (more aggressive) threshold. This is dampened by the mimetic load K, which increases with low probability of encountering a pathogen or low benefit to-cost-ratio of attacking that pathogen (low pathogenity). When m approaches zero, the dupe cannot distinguish between mimic and model and tends to attack both in the same manner ($t^* \to -\infty$).

Transferred to our model, the trait is opsonization with C3b and m is the difference in opsonization of the pathogen compared to the host. As the dupe and the model represent one entity in our model (the host), for $m \to 0$, autoreactivity may occur.

The population based evolutionary model

For the evolutionary model we assume that the C3b distribution of a given species is defined by the ability of FH surface acquisition alone. This implies that in this case all species below the FH threshold concentration t_H^* are attacked (because we assume those have a C3b opsonization above the "real" threshold regarding C3b). We next define the maximum possible binding sites the cells can produce (restricted due to limited energy and/or space), called n_{max}. Furthermore we define the relative energetic cost $c \in [0, 1]$ to produce these binding sites, compared to the total energy available to the pathogen. The overall payoff u of a species S is the product of the energy available for growth and maintenance after receptor production and its survival probability. This energy is, for simplicity's sake, assumed to depend linearly on n_S, the number of binding sites species S actually produces:

$$E_S = 1 - c\frac{n_S}{n_{max}}. \tag{12}$$

The payoff for the pathogen then reads

$$u_P = E_P(1 - a_P) \tag{13}$$

where we use the abbreviation $a_P = \mathcal{F}_P(t|p_P, n_P)$, which is the pathogen's probability of being attacked, given threshold t.

The payoff of the host H will depend on the attack decision:

$$u_H = E_H f_A(t) \tag{14}$$

If we assume that both the pathogen and the host can alter their amount of receptors and their dissociation constant and the host decides which threshold it should assign to a given pathogen (i.e. based on its degree of mimetic resemblance and on the pathogenity in general) strategies of pathogen cells are a pair (n, K_d), with $n \in \mathrm{N} = \{0, 1, \ldots, n_{max}\}$, while host strategies are a triple (n, t, K_d) with $n, t \in \mathrm{N}$. Thus, the host has one degree of freedom more than the pathogen. Note that by decreasing the threshold for pathogenic cells which can bind FH very effectively the host can avoid autoimmunity, but has to rely on other mechanisms of immune defense than the complement system.

Optimization of the parameters was done using an evolutionary algorithm [50]. Starting from random populations of 50 host individuals and 100 pathogen individuals, it simultaneously evolves both populations by mutation and selection of individuals according to the payoff-functions u_S. The opponent is chosen randomly. Pathogens are evaluated first, so they play against the hosts of the last generation. The host population is optimized using a (50 / 2 + 200) evolution strategy [50]. This means that from 50 parent individuals 200 (mutated and recombined) offspring are generated by mating of two random individuals from the parent population. The best 50 individuals are then selected to form the new host population. The pathogen population is optimized using a (100 / 1 + 1000) evolution strategy (cloning and mutation) to simulate the higher mutation rates observed in the pathogens. Termination occurs after 1000 generations.

The protein-interaction model

To investigate C3b opsonization in a single infection scenario, we have adapted a model of human complement system [45, 46] to account for FH surface acquisition of pathogens. Our adapted model focuses on the initial part of complement activation. Thus we did not consider stabilization of the C3bBb complex with properdin or formation of the TCC. Our model of initiation of the alternative pathway of complement has 28 species and 38 reactions. The parameter values of FH binding to host and pathogen surfaces were obtained by own experiments. Red blood cell data was taken from the combined NHANES datasets from 2001 to 2014 [51]. Altogether the parameter values were chosen so as to provide realistic estimates of the conditions encountered in the blood stream.

We implemented the model using the COmplex PAthway SImulator, COPASI [52]. Units of the model are micromole for amount of substance, litre for volume and milliseconds for time. C3b amplification may occur in blood plasma, serum or on surfaces. In serum it is activated by a spontaneous tick-over reaction of C3 into $C3_{H_2O}$. As $C3_{H_2O}$ has similar properties to C3b, we did not distinguish between $C3_{H_2O}$ and C3b in the model, but between fluid and surface bound molecular species (denoted by the prefixes f and b respectively). C3b will then associate with factor B (FB) to form the C3 proconvertase (C3bB), which is activated by factor D, resulting in the active C3 convertase (C3bBb). C3bBb in turn is able to convert more C3 into C3b, starting the loop again (see Fig 1).

In contrast to the spontaneous cleavage, the proteolytic cleavage of C3 into C3b results in a reactive intermediate called nascent C3b (nC3b), which can bind covalently to cell surfaces before it associates with water to form C3b [21]. Fig 3 depicts the processes around the binding of C3b on cell surfaces. The processes shown in Fig 1 are part of these and are depicted there in more detail.

If nC3b encounters a surface, the same positive feedback as in fluid may occur, where the tick-over (basal rate of spontaneous decay) is replaced by the rate of attachment of nC3b to host or pathogen surfaces (k^{+}_{nC3b}). Proteolytic cleavage of C3 by the C3 convertase assembled on surfaces (bC3bBb) will again result in nascent C3b (bnC3b). Although fnC3b and bnC3b are chemically identical, the dynamics of bnC3b surface binding in an ODE system will differ from those of fnC3b, as was already pointed out by Zewde [45]. This is because the local concentration of binding sites surrounding a bC3bBb unit will differ from the global concentration (B_{C3b}) due to spatial effects which should not be neglected (see S5 Appendix and S7 Fig). This will effectively increase the rate of bnC3b binding to their originating surfaces, compared to other surfaces or fnC3b binding.

A diagram of all reactions, as well as tables of complement concentrations and kinetic rate constants used can be found in the Supporting Information (see S2 Fig, S1 and S2 Tables).

Generally, we distinguish two cases, one where the pathogen species is not able to acquire FH on the cell surface (represented by *E. coli*) and one where the species is able to acquire FH (represented by *C. albicans* which can bind FH by the surface molecule Pra1). The host (represented by erythrocytes) can always acquire FH by heparan sulfates (HS) on the cell surface. In the case that FH can be acquired, we assume the same amount of FH binding sites compared to C3b binding sites, which is the whole surface (maximum number). This assumption is supported by the results of population based simulations (see Fig 4c).

As was already mentioned in the section on Dynamics of C3b opsonization, we included some spatial aspect into the ODE model, by assuming a higher affinity of surface derived nascent C3b to the originating surface. Derivation of the scaling factor and simulations not considering this scaling can be found in the Supporting Information (S5 Appendix and S7 Fig).

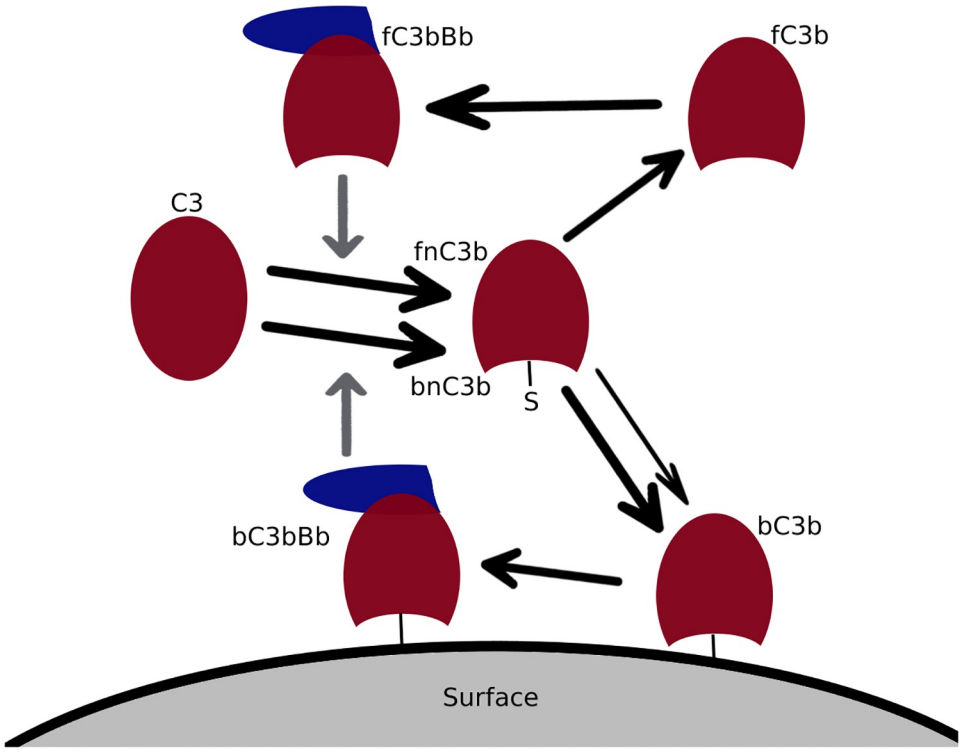

Fig 3. Scheme of C3b surface binding. Proteolytic cleavage of C3 by either fluid (denoted by the prefix f) or surface bound (denoted by the prefix b) C3 convertase (fC3bBb or bC3bBb) results in a reactive intermediate (fnC3b or bnC3b) which is able to covalently attach to surfaces due to an exposed thioester bond. While chemically there is no difference between fnC3b and bnC3b, we distinguish them in the model, because we assume a higher binding rate of bnC3b to the originating surface (see text and S5 Appendix).

https://doi.org/10.1371/journal.pone.0212187.g003

Complement factors B, D and I were fixed at their physiological concentrations (S1 Table). C3a and iC3b act as a sink in the model and were fixed at zero concentration. C3 and FH were modelled with an explicit inflow and outflow limited only by blood flow. Inflows and outflows were chosen such that the steady state corresponds to the physiological concentrations of C3 and FH. This is to prevent unrealistic behaviour, where especially C3 consumption grows infinitely due to the positive feedback loop in C3b production at high surface concentrations. A detailed description of assumptions regarding C3 and FH dynamics and sensitivity of the model with respect to these assumptions can be found in the Supporting Information (S3, S5 and S6 Figs).

During simulations, host cells were inoculated into the medium first and the system was given enough time to approach a steady state. In the case that no FH and C3 inflow occurs, the system cannot approach the physiological steady state because the initial concentrations of C3 and FH are not sufficient to cover all cells simultaneously. In this case we gave the system several C3 and FH pulses corresponding to physiological concentrations until steady state was reached (see S4 Fig for example runs).

After 1000 seconds, a pathogen is assumed to enter the bloodstream, where the concentrations of pathogenic C3b and FH (if suitable) binding sites were set to the concentrations calculated from the pathogen count defined. Final concentrations of all relevant chemical species were obtained after additional 800 seconds have passed and the system again had enough time to reach steady state (half an hour of simulation in total). Because of the pathogen arrival, we

had to use fixed time points for measurements and could not use steady-state information directly.

If distributions were available (in particular, of the erythrocyte count as well as erythrocyte and pathogen surface area, see S1 Fig), 1000 values were sampled from those distributions to obtain C3b distributions for host and pathogen cells at specified pathogen concentrations. The optimal attack threshold in terms of signalling theory was computed for distributions as described in the previous section.

Results

Population based evolutionary model

Fig 4 shows the results of the population based model if there is no restriction on parameter values. Remember that the evolutionary model uses the simplification that if FH is bound, no C3b amplification can occur. Therefore all cells with a lower amount of FH bound to the surface than the threshold are attacked in this model (gray shaded area), instead of all cells above a certain C3b threshold.

If there is no benefit in attacking the pathogen at all (in which case it is no pathogen), no cells are attacked (threshold 0) and no binding sites are produced, yielding the highest payoff (1 for pathogen and host). As soon as there is some benefit in attacking the pathogen, both the pathogen and host will start producing their maximum number of binding sites and minimizing the dissociation constant for FH. In consequence, the FH and therefore the C3b

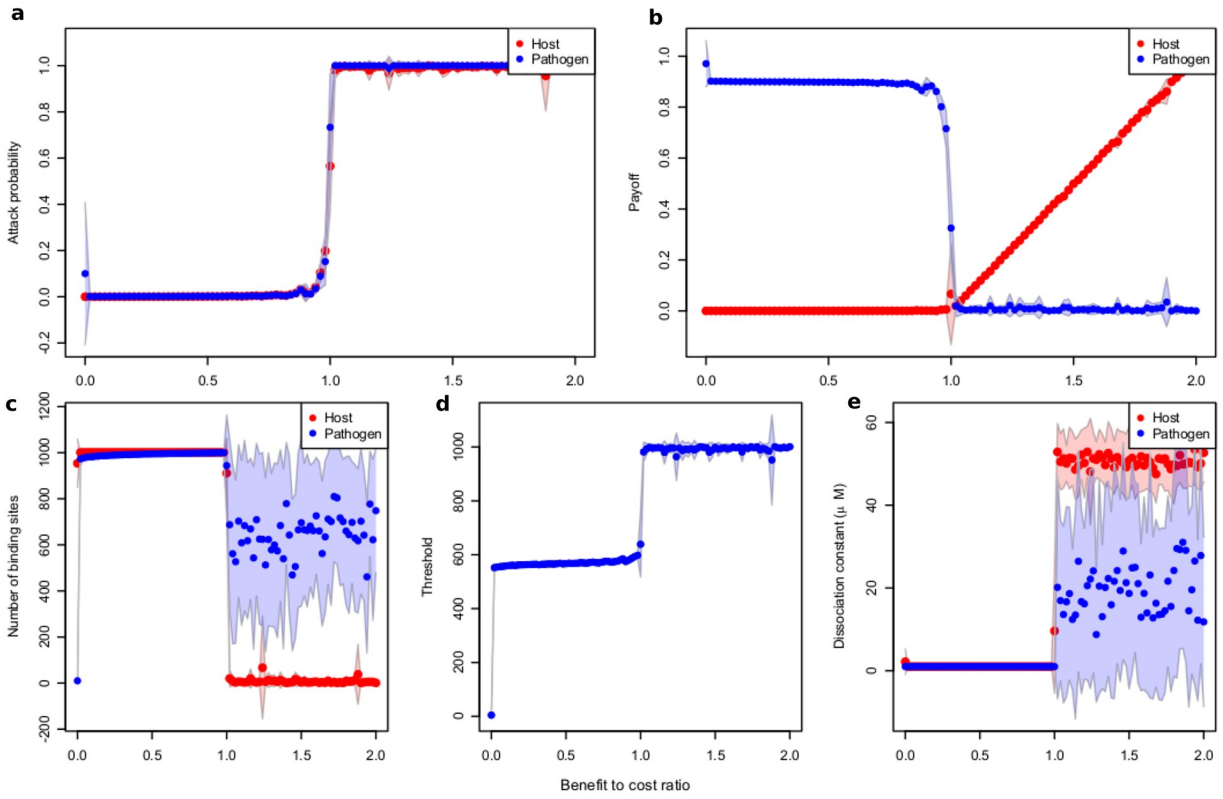

Fig 4. Plot of essential quantities as functions of the benefit-to-cost ratio, computed by numerical optimization. a) Mean probabilities of being attacked by phagocytes for pathogen and host cells. b) Payoff. c) Optimal number of binding sites. d) Classification threshold. e) Dissociation constant. Standard deviation is indicated. Maximum number of binding sites n_{max}, 1001; metabolic cost c, 0.1 for both the host and pathogens, 20 runs. FH concentration was set to 1.61 μM.

https://doi.org/10.1371/journal.pone.0212187.g004

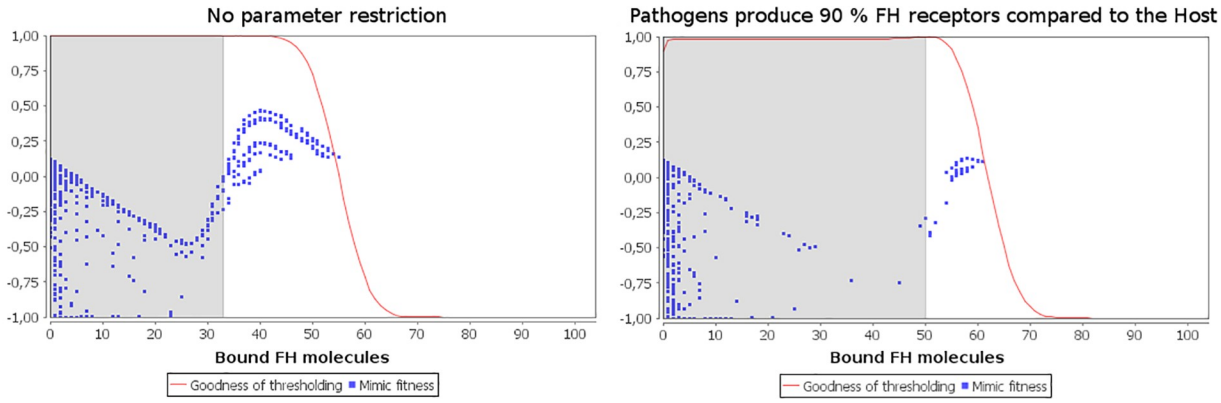

Fig 5. Plot of the fitness landscape of pathogens with fixed host parameters. Equal pathogen and host concentrations were used. Each blue dot represents one individual with a certain investment into the number of binding sites produced (x-axis location) and a certain fitness (y-axis location, determined by the attack probability solely). The red line represents the goodness of thresholding, which is the relative fitness of a host with attack threshold t, compared to the fitness of a host using the optimal attack threshold t^*. Host investment into number of binding sites is arbitrarily fixed to 40% (left) and 60% (right). In the right subfigure, pathogens are restricted to produce a maximum of 90% of host binding sites.

https://doi.org/10.1371/journal.pone.0212187.g005

distributions on the cell surface will be almost identical and the host cannot distinguish between self and non-self. This leads to a scenario where a lower number of cells are attacked if the benefit in attacking a pathogen is smaller than the cost of attacking an own cell, but all cells are attacked if it is the other way around. Note that when all cells are attacked, there is a random drift in the dissociation constant and the payoff of the host will increase linearly with r. Hosts save the cost of producing binding sites altogether in this case, while pathogens do not.

Fig 5 shows the fitness landscapes of pathogens with fixed host parameters and unlimited (A) or restricted (B) binding site production of the pathogen. In both of the scenarios, there is one local fitness maximum if no binding sites are produced at all and one global maximum at perfect (possible) resemblance. Nevertheless we can observe that the global maximum at the best possible resemblance tends towards the local one as pathogens are less able to obtain perfect resemblance (similar results are observed when restricting for example metabolic energy gain or binding effectiveness).

C. albicans opsonization

In the following, C3b opsonization means all C3b derived chemical species bound on the surface of host or pathogen. This is the sum of bC3b, bC3bB and bC3bBb concentrations.

Fig 6 shows the mean C3b opsonization per cell and sample distributions at given pathogen concentrations if factor H can be acquired by the fungus. For low *C. albicans* concentrations compared to erythrocyte concentrations (less than 10^8 *C. albicans* cells per litre, 1: 50000), host cells have less than one molecule C3b per cell bound on average, while *C. albicans* opsonization is about 10^6 molecules per cell, corresponding to the whole surface opsonized. Host opsonization then increases until a *C. albicans* concentration of $5 \cdot 10^{11}$ cells per litre is reached (ratio of 1:10 *C. albicans* vs. erythrocyte cells).

After this point, opsonization of both pathogen and host cells sharply decreases, reaching the opsonization state of the host as if no pathogen were present. The distribution at this point shows that the predicted attack threshold is high, implying very low autoreactivity but effective crypsis of a great deal of pathogens. This behaviour continues until *C. albicans* reaches nearly

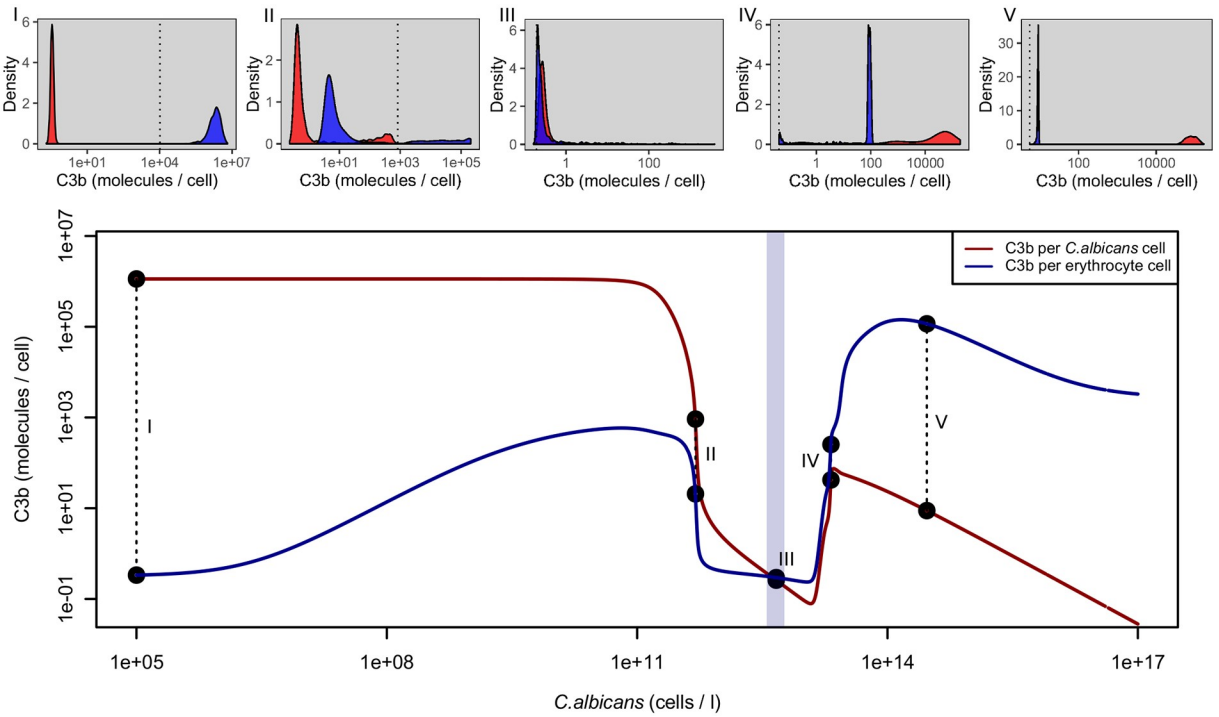

Fig 6. Computed C3b opsonization per cell if factor H can be acquired on the cell surface of the pathogen. Upper panels, distributions of opsonization for different *C. albicans* concentrations. Microbial cell densities for subfigures (I)-(V) can be seen from the corresponding points in the lower panel (see also text). The dotted vertical line in each subfigure represents the mean value of the optimal threshold interval to distinguish the two signals. Lower panel, mean opsonization on host and pathogen surfaces as functions of pathogen concentration, double logarithmic plot. Erythrocyte counts used are indicated by the light blue shaded area (mean $4.64 \cdot 10^{12}$ erythrocytes per litre, low: 1st percentile, high: 99th percentile, see S1 Fig). C3b opsonization is similar to the case where no FH can be aquired up to a *C. albicans* density of approx. $5 \cdot 10^{11}$ (i.e., erythrocytes are still 10 times more abundant). Beyond this point crypsis is successful with low opsonization in general. If the pathogen concentration increases even more, competition for factor H dominates and opsonization of both species increases with higher opsonization of host cells until the point where the inflow of C3 is not sufficient to maintain opsonization and C3b decreases again, notably faster for pathogen cells. Separability of the two signals for macrophages is only possible for low pathogen densities. At high pathogen load, the host C3b distribution is similar to the pathogen's C3b distribution at low pathogen load (subfigures (I) and (V)).

https://doi.org/10.1371/journal.pone.0212187.g006

the same concentration as the erythrocytes ($4.64 \cdot 10^{12}$). Actually the turning point (the intersection point of the red and blue curves in Fig 6) is slightly less than the mean erythrocyte concentration. Beyond this point, the signals become clearly inseparable and the predicted threshold is very low, meaning the attack of the majority of host and pathogen cells.

For even higher *C. albicans* concentrations, we observe competition for FH (see S3 Fig) and opsonization increases for both host and pathogen cells, while increasing faster for host cells. At a *C. albicans* concentration of about $2.1 \cdot 10^{13}$ (ratio of 5:1 *C. albicans* vs. erythrocyte cells) opsonization starts decreasing again for the pathogen, while opsonization of host cells still increases. After a *C. albicans* concentration of about $2.96 \cdot 10^{14}$ is reached (ratio of 65:1 *C. albicans* vs. erythrocyte cells), the C3b distributions of host and pathogen are basically transposed compared to the case where pathogens are absent or present in low numbers in the medium (subfigures (I) and (V) of Fig 6).

In the case of molecular crypsis of pathogens, the model suggests three discriminable regimes of opsonization, mainly depending on the concentration of pathogens in the blood (see Fig 7). In the first regime (low pathogen concentration), molecular crypsis is not effective and the host is able to clearly discriminate between self and non-self. In the second regime (medium pathogen concentration), molecular crypsis is successful and opsonization of host

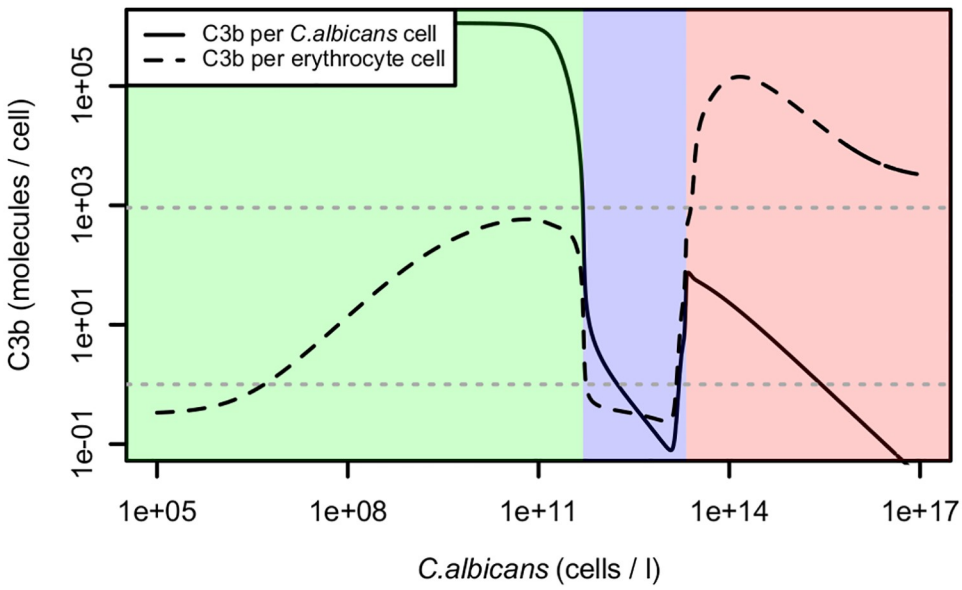

Fig 7. Mean opsonization of erythrocytes and *C. albicans* cells with different regimes and possible attack thresholds indicated. Same data as in Fig 6. The two dotted horizontal lines represent possible attack thresholds. Upper line, optimal threshold derived from simulations on *E. coli*; lower line, already a single C3b molecule is sensed on the surface. Cells with values above those lines would be attacked. Green, non-successful crypsis; blue, regime of successful crypsis; red, autoreactivity. These regimes are indicated for the upper attack threshold. Using the lower threshold, autoreactivity may occur even for low pathogen concentrations. For any of these thresholds and for any other threshold tested (see subfigures of Fig 6), host opsonization drastically increases for high pathogen concentrations, making autoreactivity nearly unavoidable.

https://doi.org/10.1371/journal.pone.0212187.g007

and pathogen is low. In the third regime (high pathogen concentration) complement is hyperactive on self, leading to autoreactivity. High autoreactivity due to high pathogen cell density is doubtless not beneficial for the host but may also not be beneficial for the pathogen [8]. It is an interesting question in this context if there are mechanisms of pathogens to avoid too high concentrations in the host system.

E. coli opsonization

Fig 8 shows the mean C3b opsonization per cell and sample distributions at given pathogen concentrations if no factor H can be acquired by the microbes. For low *E. coli* concentrations compared to erythrocyte concentrations(less than 10^8 *E. coli* cells per litre, ratio of 1: 50000), host cells have less than one molecule of C3b per cell bound on average, while *E. coli* opsonization is about 10^5 molecules per cell, corresponding to the whole surface opsonized. Distributions show clear separability of the two signals in this case. As the *E. coli* concentration increases, opsonization of the microbe remains at the maximum level and decreases only for high microbe concentrations (greater than 10^{14} cells per litre, ratio of 20:1). Host opsonization nevertheless increases to a maximum of about 1000 molecules per cell. The signals still remain clearly separable until a concentration of 10^{17} *E. coli* cells per litre is reached. This corresponds to a ratio of 20000: 1 *E. coli* cells compared to erythrocytes. Even at this high ratio, separability can be achieved, but induces some autoreactivity, as can be seen from subfigure (V) in Fig 8.

Discussion

Here, we have analysed molecular crypsis by microbial pathogens involving human factor H. In this case, crypsis is defensive and aggressive at the same time because the mimics' intention

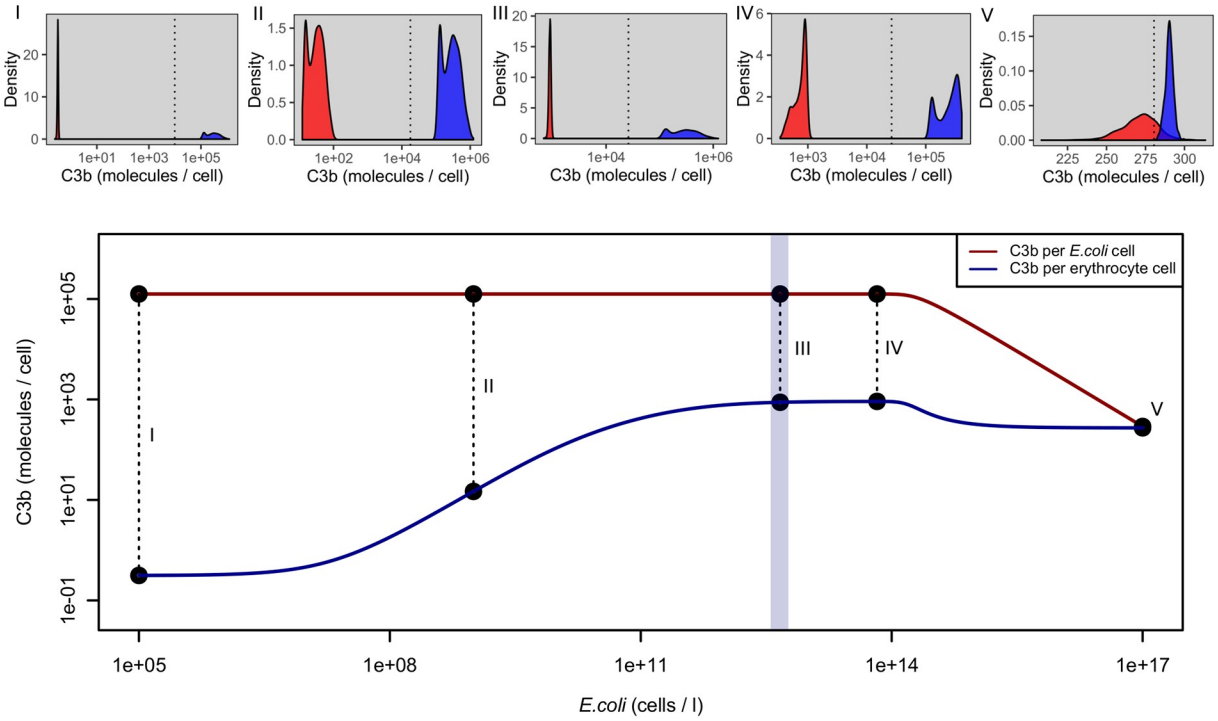

Fig 8. Computed mean C3b opsonization per cell if factor H cannot be acquired on the surface of the microbial cell. Erythrocyte counts used are indicated by the light blue shaded area (mean $4.64 \cdot 10^{12}$ erythrocytes per litre, low: 1st percentile, high: 99th percentile, see S1 Fig). Microbial cell densities for subfigures (I)-(V) can be seen from the corresponding points in the lower panel. Curves represent mean C3b deposition on host and *E. coli* surfaces (double logarithmic plot). Subfigures represent C3b distributions at several *E. coli* concentrations. The dotted vertical lines in subfigures (I)-(V) represent the mean value of the optimal threshold interval to distinguish the two signals described in the section above. C3b opsonization remains low for host cells and high for microbial cells in a wide range of microbial cell densities and the signals are mostly well separable. Only for very large microbial cell densities they become inseparable because of insufficient production of C3 (see S3 Fig).

https://doi.org/10.1371/journal.pone.0212187.g008

is invasion of unprotected host cells and mimicry makes them less suspicious, but at the same time other cell lines of the host can be regarded predators of the mimics so they need to hide from them in a defensive manner.

In particular, we established a mathematical model of molecular crypsis by *Candida albicans*. It integrates methods from signal detection and protein interaction modelling. By choosing appropriate parameter values, it is easily adaptable to be applied to other pathogens. Results were compared to a strain of *Escherichia coli* that is considered not to perform molecular crypsis using FH.

Our results indicate that if microbes cannot acquire FH on their cell surface, the alternative pathway of complement is active on microbial cells and inactive on host cells, clearly separating self from non-self over a wide range of parameters. We demonstrated that, if pathogens are able to acquire FH on their surface, the effectiveness of complement may depend substantially and highly non-linearly on the quantity (and FH binding quality) of pathogen surface in the blood. This may come as a surprise because intuitively one would expect a linear dependence of opsonization on the target surface present in the medium.

The failure of molecular crypsis to be successful at low pathogen concentrations can be explained by the fact that, due to the positive feedback loop leading to amplification of C3b, there is no pure competition between C3b and FH. Rather, it is important which of the two binds first. This corresponds to the idea that at the very start of an infection, a single molecule

of C3b encountering an unprotected surface may initiate a positive feedback loop of C3b generation (amplification) on that surface that is faster than the degradation or inactivation of C3b by surface-acquired FH. In contrast, C3b encountering a surface protected already by FH may not initiate C3b amplification. For increasing numbers of pathogen cells in the medium (injected simultaneously) the dominance of C3b amplification compared to FH acquisition may vanish as the total amount of C3 required to saturate the pathogen cell surface increases. For (temporarily) decreasing C3 levels, chances reduce that an amplification loop initiates on a pathogen surface and the speed of C3b amplification will slow down due to the short supply. The high binding affinity of FH to the pathogen surface (higher than to the host surface) may then prevent C3b amplification and ultimately lead to decomposition of all the acquired C3b, making the pathogens appear as host cells.

This result is supported by experiments performed by Stone [53]. They infused varying concentrations of 10^5 to 10^{19} *C. albicans* cells per litre at a rate of 1 ml per minute into the portal vein of mongrel dogs and measured the presence of *C. albicans* in several compartments of the blood system and other tissues after 10 minutes (see Fig 9). Their results correlate with our overall finding that clearance of mimetic pathogens is feasible at a low pathogen concentration,

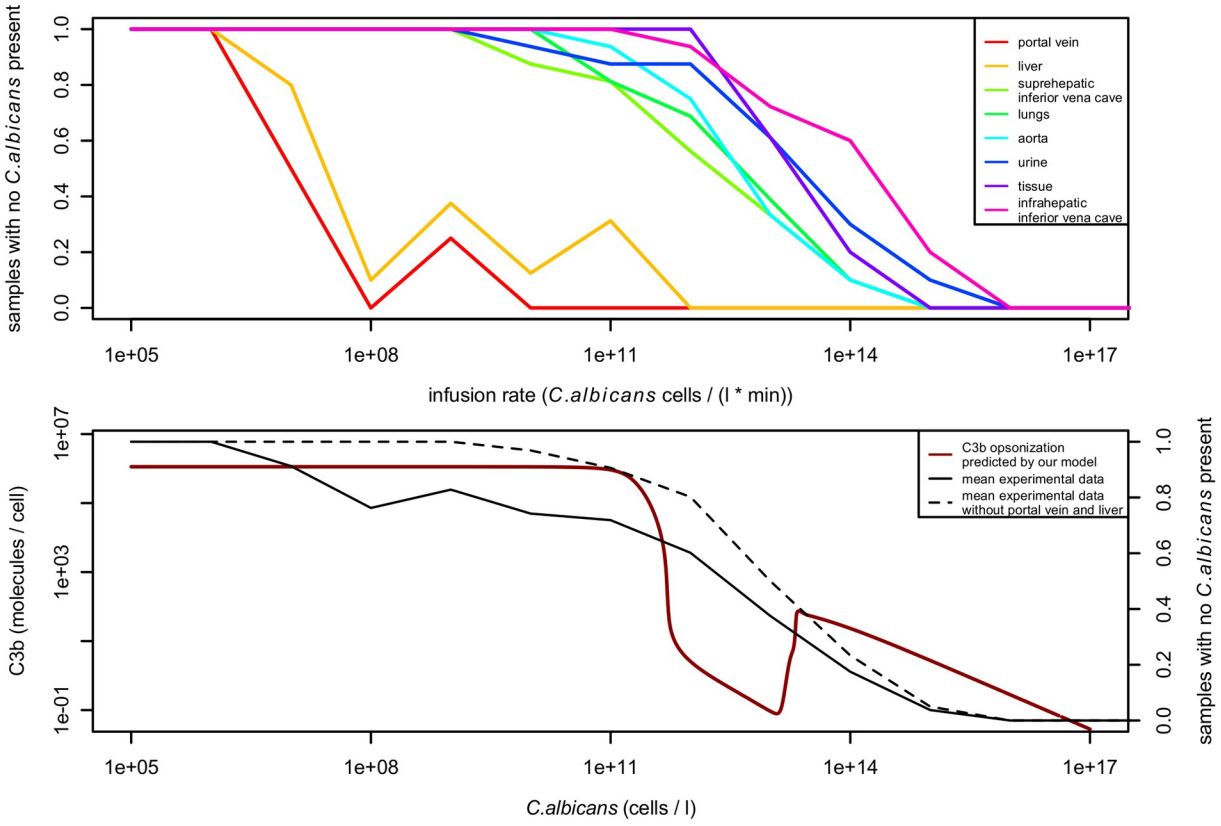

Fig 9. Effectiveness in clearing *C. albicans* cells from the blood of mongrel dogs based on varying infusion rates of *C. albicans* into the portal vein. Data was taken from Stone [53], Fig 8. Data was converted from samples positive for *C. albicans* to relative effectiveness in clearing *C. albicans* cells and scaled to units used in our model for better comparability. Top: Samples with no *C. albicans* cells present after 10 minutes, measured in different compartments of the blood system. For infusion rates below 10^{11} cells per litre per minute, *C. albicans* cells are removed to a great deal by the liver and cannot be detected in subsequent compartments of the blood system. For higher infusion rates *C. albicans* cells are present in all compartments. Bottom: Comparison to results of our model. The predicted C3b opsonization (red line) correlates to the effectiveness in clearing *C. albicans* from the blood (black lines). High opsonization means clear identifiability of mimetic pathogens and therefore easy clearance. As the predicted opsonization decreases, also a decrease in clearance of *C. albicans* cells can be observed, especially in compartments subsequent to the liver (dashed line).

https://doi.org/10.1371/journal.pone.0212187.g009

but not at a high concentration. For *C. albicans* concentrations below 10^{11} cells per litre, pathogen cells could only be detected at the infusion site and the liver. In subsequent parts of the blood system *C. albicans* was cleared successfully. For higher infusion rates nevertheless *C. albicans* was detected in all parts of the blood system. These results support our predicted transition point of the regime where molecular crypsis is not successful to the regime where it is successful, although the transition is smoother than predicted by our model and there is no increase in *C. albicans* clearing effectiveness at around 10^{14} cells per litre. This may be an artifact of the fixed C3 and FH inflow (production) rates assumed in the model, which are dynamically regulated *in vivo*.

Autoreactivity at high infusion rates was mentioned by Stone [53], but not quantified, so the transition point to the regime where autoreactivity may occur could not be compared. Note that we have not assumed, in each simulation, the *C. albicans* concentration to be time-dependent and that we have explicitly modelled the inflow of FH and C3 to regions different from the production site (the liver, see S6 Appendix).

From the above, we can conclude that the positive feedback loop of C3b amplification is beneficial for host cells in several respects. It prevents molecular crypsis from being perfect at low pathogen load and decreases the response time. It allows the host to some extent to shape the environment.

Regarding spatiality, Pangburn [22] showed that cells with activated complement and close proximity tend to "infect" each other with C3b. In our model this effect is only partially treated by increasing the rate of binding to the originating surface, but distributing the remaining increased C3b concentration to all cells in the medium (not only to cells in close proximity). If we neglect the scaling factor, we observe different results, indicating that spatiality really plays an important role (see S7 Fig). We suggest that simulations taking into account the spatial distribution and dynamics of *C. albicans* cells and erythrocytes (especially in differently sized blood vessels, like veins and capillaries), would be very helpful to fully understand the effects of molecular crypsis by pathogenic microbes. For example, the concentration of the same amount of pathogens invading a capillary will be higher compared to veins, simply because the "local" volume of capillaries is smaller than for veins. Also blood viscosity varies with the radius of the vessel [54]. Besides the different susceptibility of tissues to pathogen invasion, this could help to understand why several autoimmune diseases like age-related macular degeneration (AMD) seem to be tissue-specific.

The effect of increasing opsonization on host cells but not on *C. albicans* cells at increasing pathogen concentrations can be explained by a higher binding affinity of FH to *C. albicans* surfaces than to host surfaces. The dissociation constant of FH at *C. albicans* surfaces is in the nano-molar range, while the dissociation constant of FH at host surfaces is in the micro-molar range. So the binding of FH to *C. albicans* surfaces is stronger than to host surfaces. This means that if we assume a somehow limited FH production, the pathogen can gain a substantial advantage in FH binding. As a result it is able to sequester dissociating protection from host cells (in addition to newly produced FH molecules), leaving them unprotected regarding C3b opsonization (see S4 and S9 Figs). Of course, the actual values will depend on the maximum expression rates of FH (see S3 and S6 Figs) and its binding sites on host and pathogen surfaces (see S8 Fig).

The question remains whether the host can avoid perfect mimicry as an evasion mechanism of the pathogen. One option for the host would be to change the total amount of complement factors, which cannot be influenced by the pathogen. However, our model shows that changing these amounts does not help because the pathogen can always bind an appropriate fraction of factor H.

To respond to a decrease in the dissociation constant of FH by the pathogen, the host should do the same and could, for example, adapt the speed of C3b amplification while increasing binding affinities to FH, reaching the same balanced system but with an advantage in FH binding. Importantly, the alternative pathway of complement is not the only defence mechanism of the host. We can imagine a scenario following the so-called Red queen hypothesis [55], where (spatially related) hosts and pathogens evolve in a permanent arms race, trying to be always one step ahead of the other [56]. If one of them is not able to adapt to the advance of the other any more, it will lose the race. Maximizing binding affinities to FH nevertheless may become harder and harder in each round and is certainly limited by physical constraints and side-effects to other systems. This means that at some point, it could have been beneficial (or unavoidable) for the host to develop a completely new system of defence against mimicking pathogens.

Besides maximizing binding affinities, another way of gaining an advantage for hosts and pathogens, is the production of additional binding sites. For example C3d, a cleavage product of C3b, can provide new binding sites for FH [57]. While it is generated on the surface of pathogens capable of molecular crypsis as well (since they also utilise FH to cleave C3b), it could be a mechanism of producing binding sites faster than the pathogen, if this cleavage product binds preferentially to host surfaces. Additionally this strategy practically does not involve any costs, since C3b is already needed to ensure complement activity and is cleaved on host cell surfaces anyway. The results of the population based model clearly indicated that both the host and the pathogen adjust the binding affinities and binding sites of factor H ligands to a maximum, although binding site production involves costs.

An important prediction of our model is that that pathogens evolve to produce the same number of binding sites as hosts or none at all. This is in line with results by Holen and Johnstone [7], showing that costs of mimicry can lead to mimetic dimorphism (explaining why not all pathogens do mimicry). We observed two fitness maxima, one local maximum if no binding sites were produced at all and one global at perfect resemblance. This can be explained as follows: The benefit of mimicry is described by a constant basal growth rate minus a linear function of costs plus a saturation function above a threshold. The sum gives a non-linear function with two maxima. It does not pay at all to have a low degree of mimicry. For example, a fly being purely black or purely yellow has achieved half of the colouring of wasps but has (nearly) no mimicry effect. No mimicry is better than low mimicry, because the former is the local maximum at zero investment. The global maximum is achieved at a certain high investment (all or nothing). It is an interesting question how the global maximum could be attained during evolution, because it is difficult to explain by micro-evolution.

One way of avoiding perfect resemblance of pathogens in a population of hosts could be the utilization of polymorphisms of relevant proteins. On the host side there is the Y402H polymorphism in the FH gene and there is also a factor H like protein (FHL-1) which is an alternatively spliced product of the FH gene. It mainly consists of the first seven (of the 20) small consensus repeats (SCRs) responsible for binding. Those polymorphisms make adaptation to specific environments harder, as was already proposed by Damian [8] in its initial study on molecular mimicry due to antigen sharing by hosts and parasites. There he suspected the AB0-polymorphism, defining the human blood groups, to be a consequence of molecular mimicry. On the pathogen side, there are also polymorphisms observable. For example pathogens often have more than one FH acquiring protein (CRASP) with slightly different binding affinity and different expression levels. Those could be adaptations to host polymorphisms, but also provide some robustness of the system if one receptor type gets lost or inefficient somehow. For example, neutrophils are able to detect the *C. albicans* FH-acquiring protein Pra1 using their $\alpha_M \beta_2$ receptor [58]. By targeting the pathogen molecule directly, neutrophils

can discriminate this specific pathogen, but it is no general mechanism to avoid mimicry, as it has to be learned for each antigen and the pathogen could adapt using another FH-acquiring molecule (i.e. *C. albicans* might also use Tef1).

It remains to be studied in more detail above which C3b concentration phagocytes decide to attack cells and if this threshold is adaptable. Based on methods of signalling theory, one can calculate optimal ways of discriminating two signals, as was shown in the Methods section. Still, it is hard to quantify the benefit of correctly attacking a pathogen and the cost of erroneously attacking a host cell. Generally we can assume none of the errors to be negligible, as was shown in a previous paper [32]. If we weight both errors equally, as was done in most of the simulations, we see that at high pathogen concentrations there is no optimal decision. The model would predict for this case that all cells present in the medium should be attacked. This is clearly not the optimal response of the host. In theory, this could only be prevented by zero benefits in attacking pathogen cells or equivalently infinite costs of attacking host cells. Such benefits and costs would be, on the other hand, non-optimal for low pathogen concentrations, as they may allow infections.

It would be optimal for the host to adapt its attack threshold based on the pathogen concentration in the blood. The threshold should be shifted towards effectiveness in clearing mimetic pathogens for low pathogen concentrations and shifted towards avoidance of autoreactivity for high pathogen concentrations. Because the pathogens hide, the host can not directly sense the pathogen concentration and adjust thresholds, but it could use other clues, like blood vessel damage, indicating that a high amount of pathogens might enter and adjust the response. This context-dependant decision making could be modeled using the extended model of Holen and Johnstone [59].

In addition to changing the threshold directly by alteration of the phagocyte's predation strategy, also alteration of the binding effectiveness of FH to surfaces may be an option to control general reactiveness of complement. This is because FH removes deposited C3b from cell surfaces and thus higher binding affinity of FH to host surfaces results in better protection (calmed down complement) of host cells. On the other hand this one-sided alteration of protection of host cells will likely result in adaptation of the FH binding effectiveness of the mimic by exactly the same amount, as we showed in the population based model. So basically both distributions would shift by the same amount in the same direction, which is then mathematically equivalent of changing the attack threshold, since it affects both errors equally. So although this may have no effect on seperability of host and pathogen cells it is a way of easily adapting general aggressiveness of complement without the need for alterations in the phagocyte's predation strategy. So in fact the Y402H polymorphism could be an example of adaptation of the attack threshold, where the YY homozygote has a reduced complement reaction, while the HH homozygote may react more aggressively and the YH heterozygote is somewhere in the middle [32].

Regardless of how the attack threshold is fixed exactly, we see that in the case where there is a high concentration of pathogens performing molecular crypsis, host opsonization can reach a point where autoreactivity seems nearly unavoidable. This may have severe consequences especially in situations where the adaptive immune system is suppressed.

In such a scenario the pathogen load can hardly be regulated at all, possibly contributing to severe malfunctions of the immune system, like autoimmune diseases (in which self cells are attacked) and sepsis. Lethal sepsis can indeed occur, for example, as a consequence of a disseminated candidiasis [60]. Depending on the specific microbial environment, the host may accept the cost of a certain degree of autoreactivity in an early stage of infection to avoid pathogen concentration reaching the regime of successful crypsis. As mentioned above, there is a polymorphism Y402H in the human FH gene, where the H variant predisposes individuals to

age-related macular degeneration [31]. It is an interesting question arising from the results of our model, if the H variant of the polymorphism on the other hand could act protectively in the context of sepsis. In addition to changes in parameter values by adaptation to the disease, some values such as C3 level are likely change due to the impact of the disease or predispositions such as anemia. This is worth studying in future extensions of the model.

Also the fungus has the capability to adapt its behaviour. For example *C. albicans* is able to switch between a white and an opaque form [27–29]. Although we did not find FH-binding proteins differentially expressed between these forms in the data by [30], there is high overexpression of SAP1 in the opaque form. SAP1 has complement-component degrading function [61] and thus may promote crypsis of the opaque form. As SAP1 also causes epithelial cell damage [62], the opaque form may be especially involved in invasion of the blood or tissue where the C3b degrading function would cause an initial depletion of C3b, increasing the chances of successful invasion. At 37˚C the fungus will switch to the white form [29], which is the predominant form in disseminated candidias [28]. To analyse white-opaque switching in the model, it could be extended to include SAP1 production of *C. albicans*. The spontaneous type-switching could be modelled using a rate constant on the population level, where SAP1 production would be increased proportional to the amount of opaque cells in the population. The initial ratio of opaque to white cells could be chosen to represent the ratio of the originating compartment (the opaque type is a better colonizer of the skin), where the equilibrium ratio in the blood will be determined by the switching rate at 37˚C, which is around 10^{-3} (1000 white on 1 opaque) [29].

Returning to the analogy of the Captain of Koepenick [4], it is worth noting that to distinguish true from false policemen, also other signals are needed, such as correct commands. The deception by the Captain of Koepenick was so perfect because he had learned and used the army commands. To avoid a perfect camouflage, the human adaptive immune system is used in addition to the innate immune system to recognize antigens as further signals for discrimination. For molecular mimicry to be successful, pathogens need to deceive both systems.

Supporting information

S1 Fig. Surface area distributions and erythrocyte count distribution used for sampling.
(PDF)

S2 Fig. Diagram of all reactions occurring in the *C. albicans* model.
(PDF)

S3 Fig. Opsonization states and relevant complement factor concentrations assuming inflow of C3 and FH limited only by blood flow.
(PDF)

S4 Fig. Example dynamics assuming inflow of C3 and FH limited only by blood flow.
(PDF)

S5 Fig. Opsonization states and relevant complement factor concentrations assuming unlimited inflow of C3 and FH.
(PDF)

S6 Fig. Opsonization states and relevant complement factor concentrations assuming no inflow of C3 and FH.
(PDF)

S7 Fig. Opsonization states and relevant complement factor concentrations without the scaling factor accounting for spatial effects.
(PDF)

S8 Fig. Opsonization states and relevant complement factor concentrations with higher heparan sulfate concentration and lower Pra1 concentration on the surfaces.
(PDF)

S9 Fig. Example dynamics assuming no inflow of C3 and FH.
(PDF)

S1 Table. Complement protein concentrations used in the model.
(PDF)

S2 Table. Kinetic rate constants used in the model.
(PDF)

S1 Appendix. C3b diffusion in the blood.
(PDF)

S2 Appendix. Binding rate of reactive C3b.
(PDF)

S3 Appendix. Decay rate of reactive C3b.
(PDF)

S4 Appendix. C3b active hemispheric region.
(PDF)

S5 Appendix. Scaling factor for the affinity of surface derived nascent C3b to the originating surface.
(PDF)

S6 Appendix. Inflow and outflow of relevant complement factors C3 and H in the blood stream.
(PDF)

S7 Appendix. The complete ODE model.
(PDF)

S8 Appendix. Supporting references.
(PDF)

Acknowledgments

Financial support by the German Research Foundation (DFG) within the Jena School for Microbial Communication (grant no. DFG-GSC 214/2) and the Transregio 124 (FungiNet, projects B1, C4 and C6) is gratefully acknowledged.

Author Contributions

Conceptualization: Christina Glock, Christine Skerka, Peter F. Zipfel, Stefan Schuster.

Data curation: Stefan N. Lang, Sebastian Germerodt, Christine Skerka, Peter F. Zipfel.

Formal analysis: Stefan N. Lang, Christina Glock.

Methodology: Stefan N. Lang, Christina Glock, Stefan Schuster.

Project administration: Christine Skerka, Peter F. Zipfel, Stefan Schuster.

Software: Stefan N. Lang.

Supervision: Christine Skerka, Peter F. Zipfel, Stefan Schuster.

Visualization: Stefan N. Lang, Sebastian Germerodt.

Writing – original draft: Stefan N. Lang, Stefan Schuster.

Writing – review & editing: Stefan N. Lang, Sebastian Germerodt, Christine Skerka, Peter F. Zipfel, Stefan Schuster.

References

1. Zabka H, Tembrock G. Mimicry and crypsis-a behavioural approach to classification. Behavioural processes. 1986; 13(1):159–176. https://doi.org/10.1016/0376-6357(86)90023-9 PMID: 24924869
2. Pasteur G. A classificatory review of mimicry systems. Annual Review of Ecology and Systematics. 1982; 13(1):169–199. https://doi.org/10.1146/annurev.es.13.110182.001125
3. Vane-Wright RI. A unified classification of mimetic resemblances. Biological Journal of the Linnean Society. 1976; 8(1):25–56. https://doi.org/10.1111/j.1095-8312.1976.tb00240.x
4. Zuckmayer C. The Captain of Köpenick: A Modern Fairy Tale in Three Acts, translated by Portman D., London. 1932.
5. Dittrich W, Gilbert F, Green P, Mcgregor P, Grewcock D. Imperfect mimicry: a pigeon's perspective. Proceedings of the Royal Society of London B: Biological Sciences. 1993; 251(1332):195–200. https://doi.org/10.1098/rspb.1993.0029
6. Huheey JE. Mathematical models of mimicry. American Naturalist. 1988; p. S22–S41. https://doi.org/10.1086/284765
7. Holen ØH, Johnstone RA. The evolution of mimicry under constraints. The American Naturalist. 2004; 164(5):598–613. https://doi.org/10.1086/424972 PMID: 15540150
8. Damian RT. Molecular Mimicry: Antigen Sharing by Parasite and Host and Its Consequences. The American Naturalist. 1964; 98(900):129–149. https://doi.org/10.1086/282313
9. Damian R. Molecular mimicry: parasite evasion and host defense. In: Molecular Mimicry. Springer; 1989. p. 101–115.
10. Tsonis PA, Dwivedi B. Molecular mimicry: structural camouflage of proteins and nucleic acids. Biochimica et Biophysica Acta (BBA)-Molecular Cell Research. 2008; 1783(2):177–187. https://doi.org/10.1016/j.bbamcr.2007.11.001
11. Blank M, Barzilai O, Shoenfeld Y. Molecular mimicry and auto-immunity. Clinical Reviews in Allergy & Immunology. 2007; 32(1):111–118. https://doi.org/10.1007/BF02686087
12. Cusick MF, Libbey JE, Fujinami RS. Molecular mimicry as a mechanism of autoimmune disease. Clinical Reviews in Allergy & Immunology. 2012; 42(1):102–111. https://doi.org/10.1007/s12016-011-8294-7
13. Oldstone MB. Molecular mimicry and immune-mediated diseases. The FASEB Journal. 1998; 12(13): 1255–1265. https://doi.org/10.1096/fasebj.12.13.1255 PMID: 9761770
14. Meri T, Hartmann A, Lenk D, Eck R, Würzner R, Hellwage J, et al. The yeast *Candida albicans* binds complement regulators factor H and FHL-1. Infection and Immunity. 2002; 70(9):5185–5192. https://doi.org/10.1128/IAI.70.9.5185-5192.2002 PMID: 12183569
15. Sharp JA, Echague CG, Hair PS, Ward MD, Nyalwidhe JO, Geoghegan JA, et al. *Staphylococcus aureus* surface protein SdrE binds complement regulator factor H as an immune evasion tactic. PloS one. 2012; 7(5):e38407. https://doi.org/10.1371/journal.pone.0038407 PMID: 22675461
16. Haupt K, Kraiczy P, Wallich R, Brade V, Skerka C, Zipfel PF. Binding of human factor H-related protein 1 to serum-resistant *Borrelia burgdorferi* is mediated by borrelial complement regulator-acquiring surface proteins. Journal of Infectious Diseases. 2007; 196(1):124–133. https://doi.org/10.1086/518509 PMID: 17538892
17. Kraiczy P, Skerka C, Kirschfink M, Brade V, Zipfel PF. Immune evasion of *Borrelia burgdorferi* by acquisition of human complement regulators FHL-1/reconectin and Factor H. European Journal of Immunology. 2001; 31(6):1674–1684 PMID: 11385611

18. Hellwage J, Meri T, Heikkilä T, Alitalo A, Panelius J, Lahdenne P, et al. The complement regulator factor H binds to the surface protein OspE of *Borrelia burgdorferi*. Journal of Biological Chemistry. 2001; 276(11):8427–8435. https://doi.org/10.1074/jbc.M007994200 PMID: 11113124

19. Blom AM, Hallström T, Riesbeck K. Complement evasion strategies of pathogens—acquisition of inhibitors and beyond. Molecular Immunology. 2009; 46(14):2808–2817. https://doi.org/10.1016/j.molimm.2009.04.025 PMID: 19477524

20. Zipfel PF, Skerka C. Complement: The Alternative Pathway. eLS. 2015.

21. Sim R, Twose T, Paterson D, Sim E. The covalent-binding reaction of complement component C3. Biochemical Journal. 1981; 193(1):115–127. https://doi.org/10.1042/bj1930115 PMID: 7305916

22. Pangburn MK, Müller-Eberhard HJ. The alternative pathway of complement. Springer Semin Immunopathol. 1984; 7(2-3):163–192. https://doi.org/10.1007/BF01893019 PMID: 6238433

23. Lambris JD, Ricklin D, Geisbrecht BV. Complement evasion by human pathogens. Nature Reviews Microbiology. 2008; 6(2):132–142. https://doi.org/10.1038/nrmicro1824 PMID: 18197169

24. Zipfel PF, Skerka C. Complement regulators and inhibitory proteins. Nature Reviews Immunology. 2009; 9(10):729–740. https://doi.org/10.1038/nri2620 PMID: 19730437

25. Ferreira VP, Pangburn MK, Cortés C. Complement control protein factor H: the good, the bad, and the inadequate. Molecular Immunology. 2010; 47(13):2187–2197. https://doi.org/10.1016/j.molimm.2010.05.007 PMID: 20580090

26. Uhlén M, Fagerberg L, Hallström BM, Lindskog C, Oksvold P, Mardinoglu A, et al. Tissue-based map of the human proteome. Science. 2015; 347(6220):1260419. https://doi.org/10.1126/science.1260419 PMID: 25613900

27. Slutsky B, Staebell M, Anderson J, Risen L, Pfaller M, Soll DR. "White-opaque transition": a second high-frequency switching system in Candida albicans. Journal of Bacteriology. 1987; 169(1):189–197. https://doi.org/10.1128/jb.169.1.189-197.1987 PMID: 3539914

28. Sasse C, Hasenberg M, Weyler M, Gunzer M, Morschhäuser J. White-opaque switching of Candida albicans allows immune evasion in an environment-dependent fashion. Eukaryotic cell. 2013; 12(1): 50–58. https://doi.org/10.1128/EC.00266-12 PMID: 23125350

29. Soll DR. Why does Candida albicans switch? FEMS Yeast Research. 2009; 9(7):973–989. https://doi.org/10.1111/j.1567-1364.2009.00562.x PMID: 19744246

30. Lan CY, Newport G, Murillo LA, Jones T, Scherer S, Davis RW, et al. Metabolic specialization associated with phenotypic switching in Candida albicans. Proceedings of the National Academy of Sciences. 2002; 99(23):14907–14912. https://doi.org/10.1073/pnas.232566499

31. Hageman GS, Anderson DH, Johnson LV, Hancox LS, Taiber AJ, Hardisty LI, et al. A common haplotype in the complement regulatory gene factor H (HF1/CFH) predisposes individuals to age-related macular degeneration. Proceedings of the National Academy of Sciences of the United States of America. 2005; 102(20):7227–7232. https://doi.org/10.1073/pnas.0501536102 PMID: 15870199

32. Hummert S, Glock C, Lang S, Hummert C, Skerka C, Zipfel PF, et al. Playing 'hide-and-seek' with factor H: Game-theoretical analysis of a single nucleotide polymorphism. 2017.

33. Zipfel PF, Hallström T, Riesbeck K. Human complement control and complement evasion by pathogenic microbes—tipping the balance. Molecular Immunology. 2013; 56(3):152–160. https://doi.org/10.1016/j.molimm.2013.05.222 PMID: 23810413

34. Jacob A, Hack B, Bai T, Brorson JR, Quigg RJ, Alexander JJ. Inhibition of C5a receptor alleviates experimental CNS lupus. Journal of Neuroimmunology. 2010; 221(1-2):46–52. https://doi.org/10.1016/j.jneuroim.2010.02.011 PMID: 20207017

35. Liu B, Zhang J, Tan PY, Hsu D, Blom AM, Leong B, et al. A computational and experimental study of the regulatory mechanisms of the complement system. PLoS Computational Biology. 2011; 7(1): e1001059. https://doi.org/10.1371/journal.pcbi.1001059 PMID: 21283780

36. Dühring S, Germerodt S, Skerka C, Zipfel PF, Dandekar T, Schuster S. Host-pathogen interactions between the human innate immune system and *Candida albicans*—Understanding and modeling defense and evasion strategies. Frontiers in Microbiology. 2015; 6:625. https://doi.org/10.3389/fmicb.2015.00625 PMID: 26175718

37. Anderson RM, May R. Coevolution of hosts and parasites. Parasitology. 1982; 85(2):411–426. https://doi.org/10.1017/S0031182000055360 PMID: 6755367

38. Hummert S, Bohl K, Basanta D, Deutsch A, Werner S, Theißen G, et al. Evolutionary game theory: cells as players. Molecular BioSystems. 2014; 10(12):3044–3065. https://doi.org/10.1039/c3mb70602h PMID: 25270362

39. Dühring S, Ewald J, Germerodt S, Kaleta C, Dandekar T, Schuster S. Modelling the host—pathogen interactions of macrophages and *Candida albicans* using Game Theory and dynamic optimization.

Journal of The Royal Society Interface. 2017; 14(132):20170095. https://doi.org/10.1098/rsif.2017.0095

40. Becker DJ, Streicker DG, Altizer S. Using host species traits to understand the consequences of resource provisioning for host—parasite interactions. Journal of Animal Ecology. 2018; 87(2):511–525. https://doi.org/10.1111/1365-2656.12765 PMID: 29023699

41. Speed MP, Ruxton GD. Imperfect Batesian mimicry and the conspicuousness costs of mimetic resemblance. The American Naturalist. 2010; 176(1):E1–E14. https://doi.org/10.1086/652990 PMID: 20497052

42. Huheey JE. Studies in warning coloration and mimicry. VII. Evolutionary consequences of a Batesian-Müllerian spectrum: a model for Müllerian mimicry. Evolution. 1976; p. 86–93. https://doi.org/10.1111/j.1558-5646.1976.tb00884.x PMID: 28565050

43. Speed MP. Muellerian mimicry and the psychology of predation. Animal Behaviour. 1993; 45(3):571–580. https://doi.org/10.1006/anbe.1993.1067

44. Markiewski MM, DeAngelis RA, Lambris JD. Complexity of complement activation in sepsis. Journal of Cellular and Molecular Medicine. 2008; 12(6a):2245–2254. https://doi.org/10.1111/j.1582-4934.2008.00504.x PMID: 18798865

45. Zewde N, Gorham RD Jr, Dorado A, Morikis D. Quantitative modeling of the alternative pathway of the complement system. PloS one. 2016; 11(3):e0152337. https://doi.org/10.1371/journal.pone.0152337 PMID: 27031863

46. Korotaevskiy AA, Hanin LG, Khanin MA. Non-linear dynamics of the complement system activation. Mathematical Biosciences. 2009; 222(2):127–143. https://doi.org/10.1016/j.mbs.2009.10.003 PMID: 19854207

47. Wooster DG, Maruvada R, Blom AM, Prasadarao NV. Logarithmic phase Escherichia coli K1 efficiently avoids serum killing by promoting C4bp-mediated C3b and C4b degradation. Immunology. 2006; 117(4):482–493. https://doi.org/10.1111/j.1365-2567.2006.02323.x PMID: 16556262

48. Wiley RH. Errors, exaggeration, and deception in animal communication. Behavioral Mechanisms in Evolutionary Ecology. 1994; p. 157–189.

49. Yanes RE, Gustafson CE, Weyand CM, Goronzy JJ. Lymphocyte generation and population homeostasis throughout life. Seminars in Hematology. 2017; 54(1):33–38. https://doi.org/10.1053/j.seminhematol.2016.10.003 PMID: 28088985

50. Beyer HG, Schwefel HP. Evolution strategies—A comprehensive introduction. Natural Computing. 2002; 1(1):3–52. https://doi.org/10.1023/A:1015059928466

51. Centers for Disease Control and Prevention (CDC) National Center for Health Statistics (NCHS). National Health and Nutrition Examination Survey Data. Hyattsville, MD: US Department of Health and Human Services, Centers for Disease Control and Prevention. 2001-2014;.

52. Hoops S, Sahle S, Gauges R, Lee C, Pahle J, Simus N, et al. COPASI—a complex pathway simulator. Bioinformatics. 2006; 22(24):3067–3074. https://doi.org/10.1093/bioinformatics/btl485 PMID: 17032683

53. Stone HH, Kolb LD, Currie CA, Geheber CE, Cuzzell JZ. Candida sepsis: pathogenesis and principles of treatments. Annals of surgery. 1974; 179(5):697. https://doi.org/10.1097/00000658-197405000-00024 PMID: 4207351

54. Pries AR, Neuhaus D, Gaehtgens P. Blood viscosity in tube flow: dependence on diameter and hematocrit. American Journal of Physiology—Heart and Circulatory Physiology. 1992; 263(6):H1770–H1778. https://doi.org/10.1152/ajpheart.1992.263.6.H1770

55. Brockhurst MA, Koskella B. Experimental coevolution of species interactions. Trends in Ecology & Evolution. 2013; 28(6):367–375. https://doi.org/10.1016/j.tree.2013.02.009

56. Lively CM, Dybdahl MF. Parasite adaptation to locally common host genotypes. Nature. 2000; 405(6787):679–681. https://doi.org/10.1038/35015069 PMID: 10864323

57. Perkins SJ, Fung KW, Khan S. Molecular interactions between complement factor H and its heparin and heparan sulfate ligands. Frontiers in immunology. 2014; 5. https://doi.org/10.3389/fimmu.2014.00126 PMID: 24744754

58. Soloviev DA, Jawhara S, Fonzi WA. Regulation of innate immune response to Candida albicans infections by $\alpha_M\beta_2$-Pra1p interaction. Infection and immunity. 2011; 79 4:1546–58. https://doi.org/10.1128/IAI.00650-10 PMID: 21245270

59. Holen i, Johnstone R. Context-Dependent Discrimination and the Evolution of Mimicry. The American Naturalist. 2006; 167(3):377–389. https://doi.org/10.1086/499567 PMID: 16673346

60. Spellberg B, Ibrahim AS, Edwards JE Jr, Filler SG. Mice with disseminated candidiasis die of progressive sepsis. The Journal of infectious diseases. 2005; 192(2):336–343. https://doi.org/10.1086/430952 PMID: 15962230

61. Gropp K, Schild L, Schindler S, Hube B, Zipfel PF, Skerka C. The yeast Candida albicans evades human complement attack by secretion of aspartic proteases. Molecular Immunology. 2009; 47(2): 465–475. https://doi.org/10.1016/j.molimm.2009.08.019 PMID: 19880183

62. Schaller M, Bein M, Korting HC, Baur S, Hamm G, Michel M, et al. The secreted aspartyl proteinases Sap1 and Sap2 cause tissue damage in an in vitro model of vaginal candidiasis based on reconstituted human vaginal epithelium. Infection and immunity. 2003; 71 6:3227–34. https://doi.org/10.1128/IAI.71.6.3227-3234.2003 PMID: 12761103